

SixTrack studies for Crab Cavity Failures in HL-LHC

Bruce Yee Rendón

Departamento de Física
Centro de Investigación y de Estudios Avanzados
del Instituto Politécnico Nacional Unidad Zacatenco

Scheme

- Introduction
- Results
- Summary

CC

A device called “crab cavity” (CC) applies a tiny sideways kick to each particle bunch in order to change its dynamics to achieve a head-on collision at the IP. For the HL-LHC the peak of the luminosity will be increased by factor of 10 (with respect to the nominal).

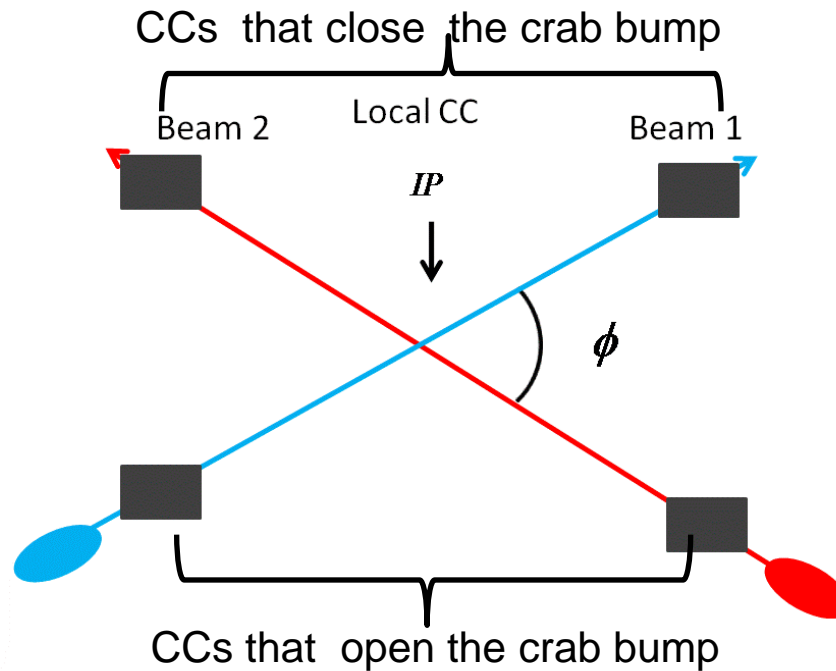


Figure 1 . The effect of the CC in the beam at interaction point in the LCC scheme.

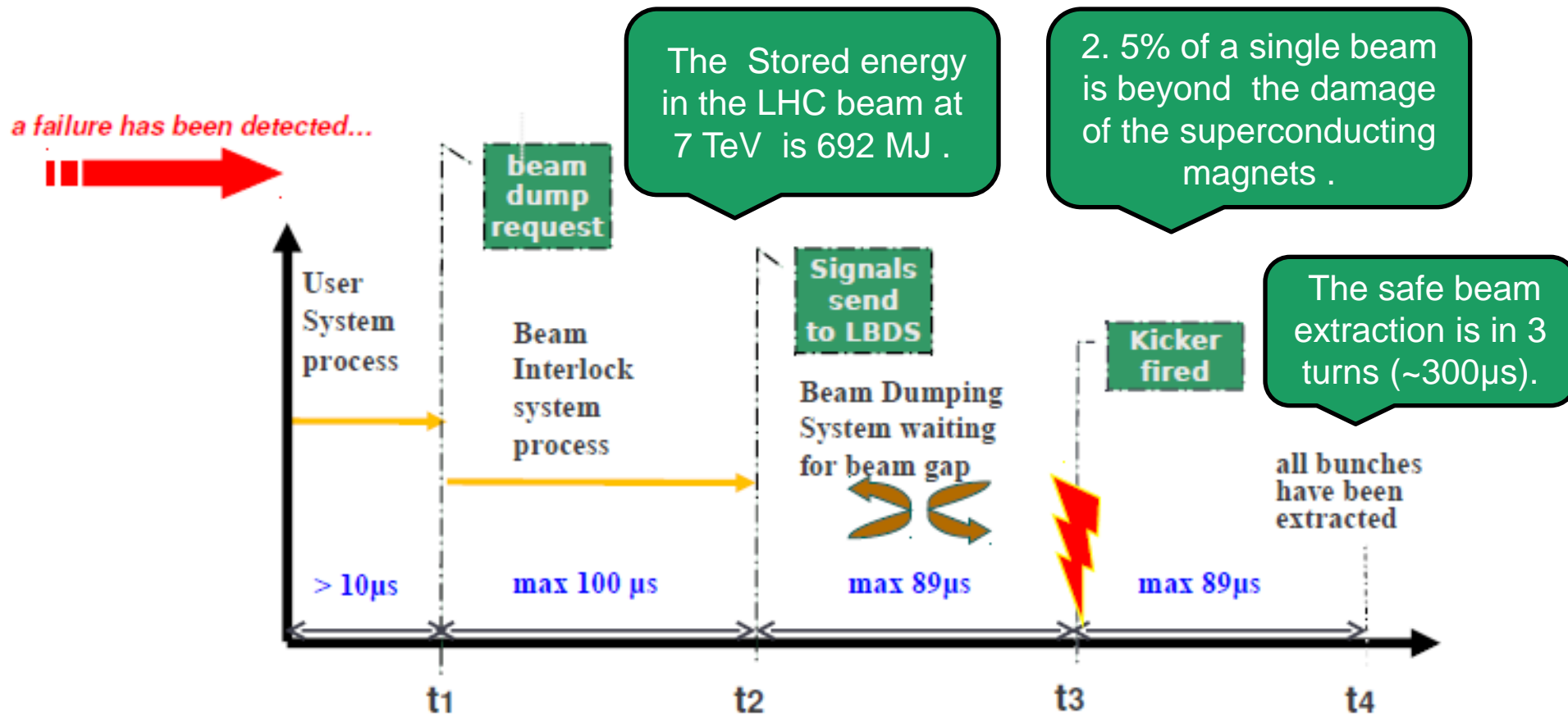
HL-LHC

optics parameters

TABLE I: Relevant optics parameters of HL-LHC under study.

Parameters	Value
Energy [TeV]	7
Protons/bunch [10^{11}]	2.2
Bunches	2808
rms bunch length [cm]	7.55
β function at IP1, 5 [m]	0.15
Normalized Emittance [μmrad]	3.75
Full crossing angle [μrad]	590

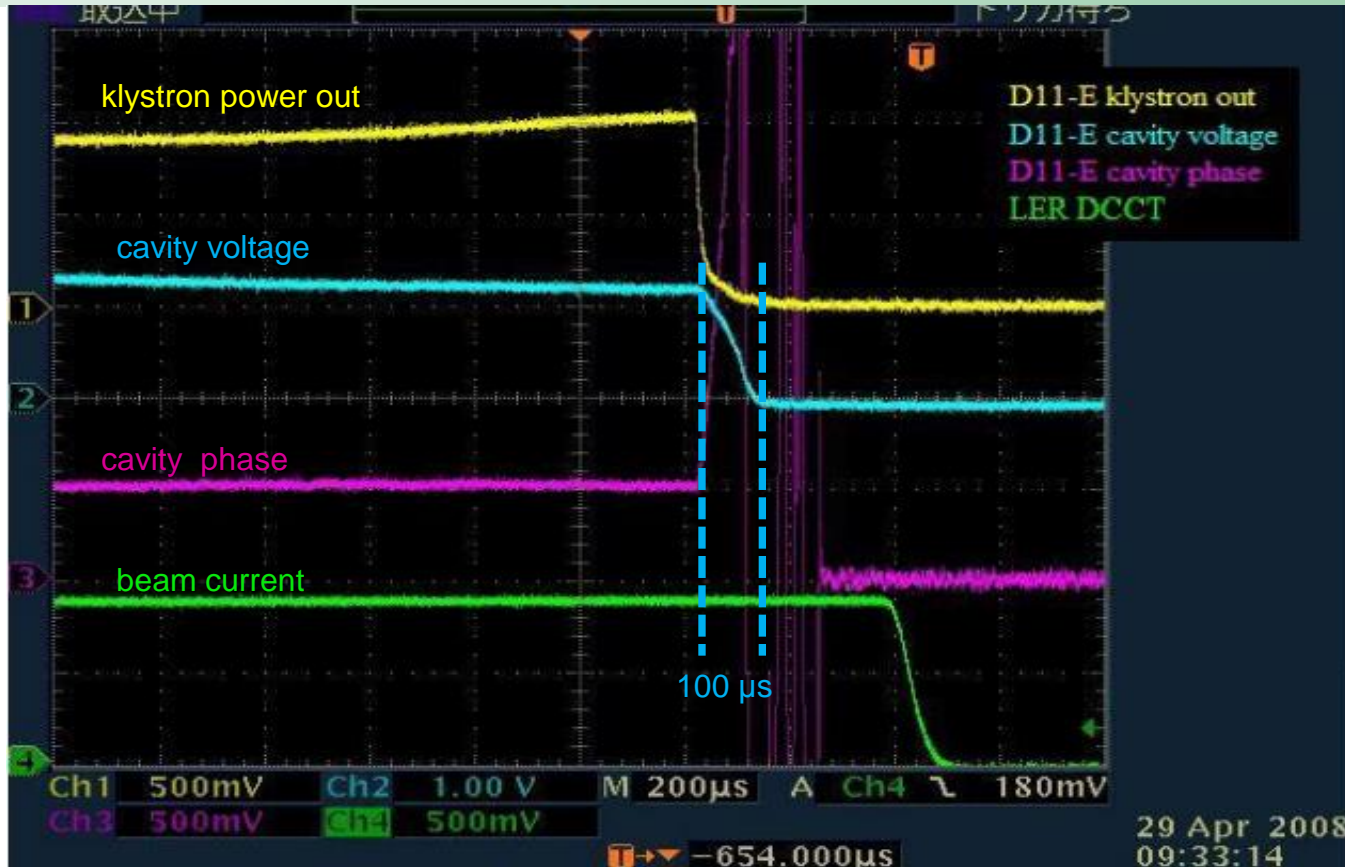
LHC safe operation



Courtesy J. Wenniger

Figure 2: Sequence of a failure detection and full beam extraction in the LHC.

CC failure at KEKB



Courtesy K. Nakanishi

Figure 3: Crab Cavity failures at KEKB. The cavity voltage decay to zero after 100 μs (~ 1 LHC turn).

- Collimation system is designed to protect the LHC lattice from unwanted beam losses.
- We used the Collimations tools to evaluate the beam losses produce by the CCs failures. The losses can be classified as :
 - A) Particle absorbed in the Collimators (TCPs, TCSGs, etc).
 - B) Particle absorbed in the aperture of the LHC lattice (cold magnets, warm magnets, etc).

Layout of the CC

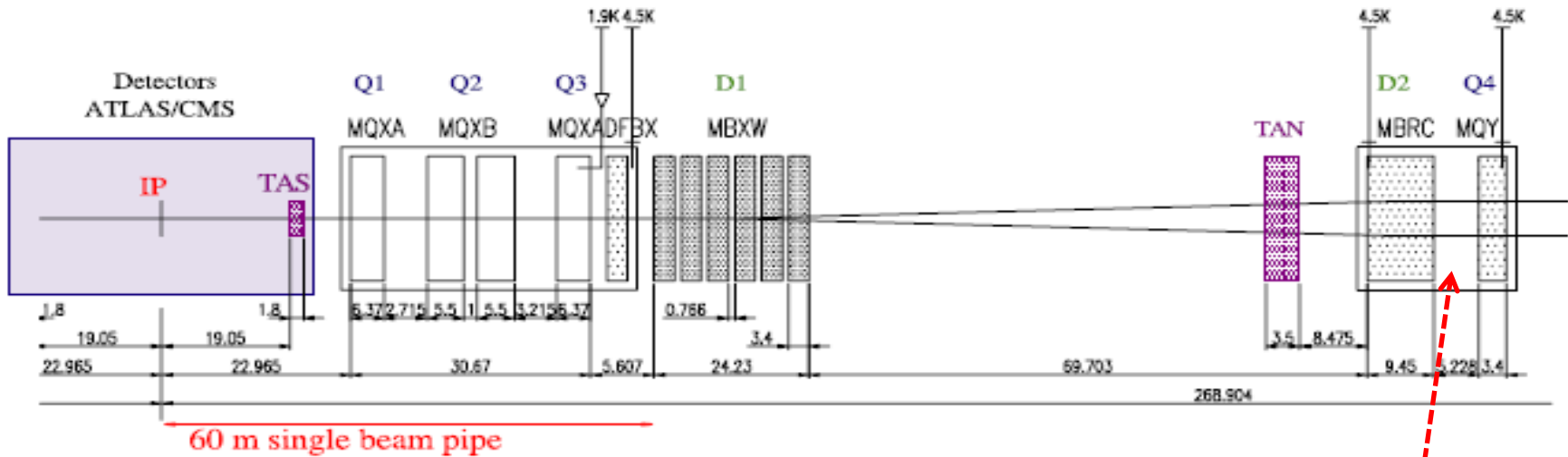
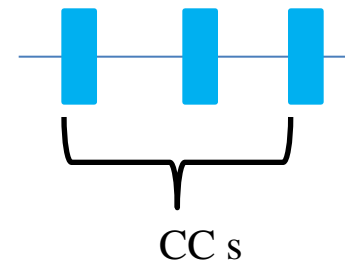


Figure 4 . Scheme layout at the right side of the IP for the LHC .

TABLE II: The CCs settings used for this studies .

IP	Frequency (MHz)	Voltage (MV)
IP1	400.7	3.5-3.8
IP5	400.7	3.8



CC operation

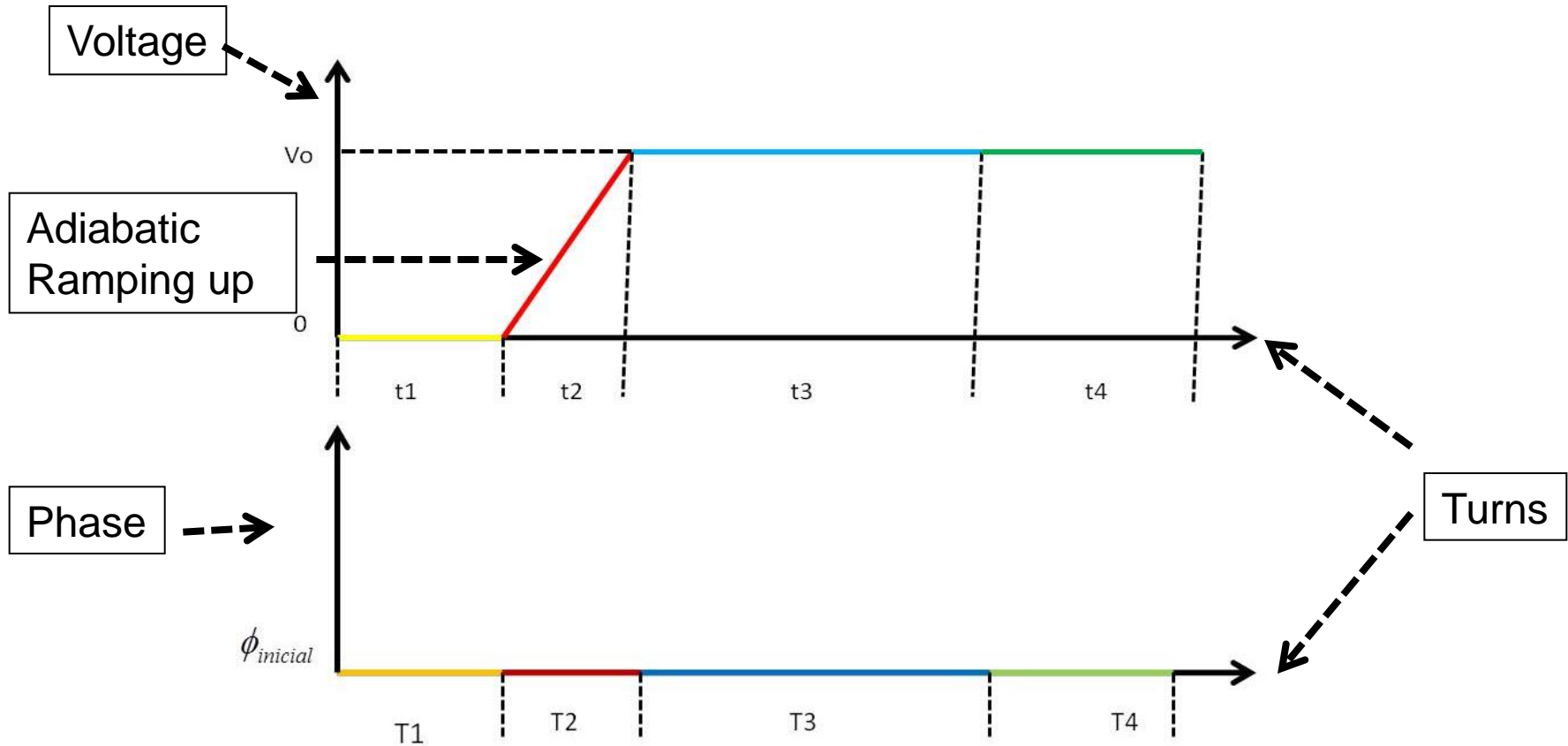


Figure 5. Normal operation represent the ideal performance of the CC.

Crab plane

- The CCs tilt the bunch in the transverse plane to achieve a head-on collision: The horizontal plane at CMS (IP5) and vertical plane at ATLAS (IP1).
- This study is with emphasis in the losses at horizontal plane, therefore, the failures is just produce in one of the CCs which close the bump at CMS. The CCs at IP1 were turn off in all the simulations.
- A study with CCs working in both planes were realized by F. Bouly*.

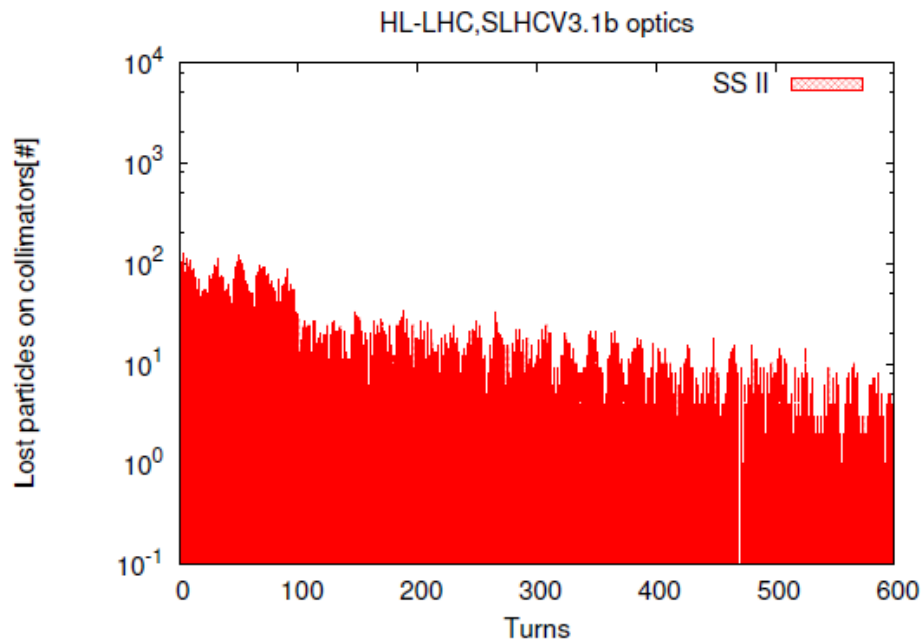
*F. Bouly. Sixtrack simulations for the study of Crab cavity failures in HL-LHC, LBS #48, 2013.

- A studies of the maximal displacement were realized by T. Baer * found that maximal displacement for a CCs failure in voltage or phase was around $2.1\sigma_x$ at $2.4\sigma_z$ position for voltage and $0\sigma_z$ for phase (for a $Q_{\text{ext}} = 1 \times 10^6$).
- In our CCs failures we found a maximal displacement $1.6\sigma_x$ at $2.4\sigma_z$ for the voltage and $2.2\sigma_x$ at $0\sigma_z$ for phase.

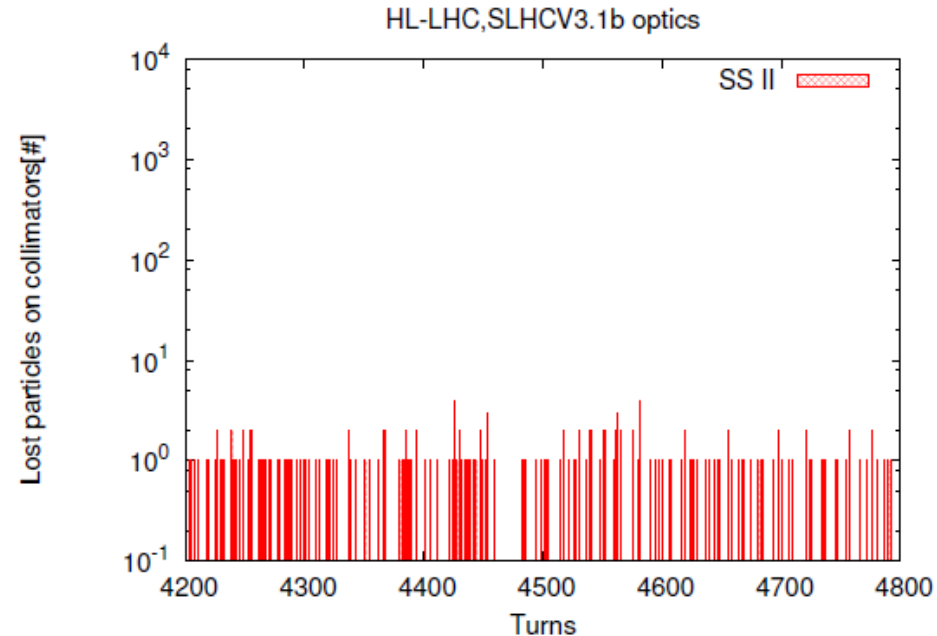
*T. Bear et al. Very Fast LHC Crab Cavity Failures and their Mitigations, 2012.

Beam distributions

- A new 2D Gaussian with matching conditions were used to generated the beam distribution.
- Two kind of halo distributions were implemented and studied:
 - a) Tiny halo : Horizontal halo at different positions with a smear of 0.1σ , a complete vertical and longitudinal beam distribution.
 - b) Thick halo: Horizontal and vertical halo with different smears and with a complete beam distribution in the longitudinal phase space.



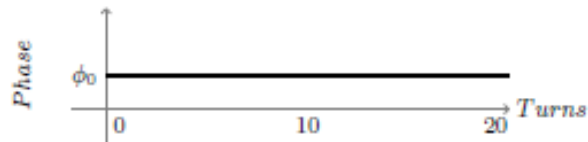
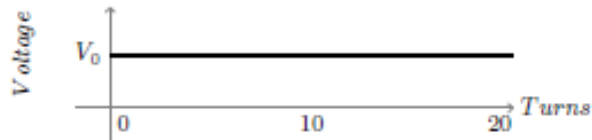
First 600 turns of the tracking.



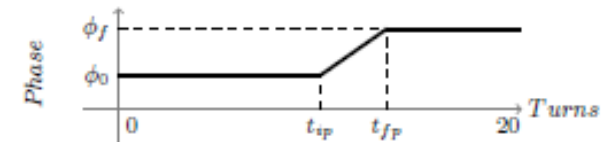
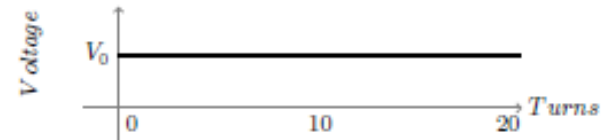
The last 600 turns of the tracking.

Figure 6. The histogram of the lost particles in the collimators for the first and last turns of the tracking to reach a realistic steady-state for the beam distributions. Most of the particles are absorbed at TCP.C6L7.B1.

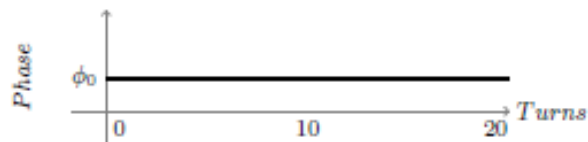
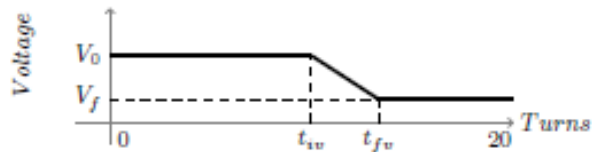
CC operation cases



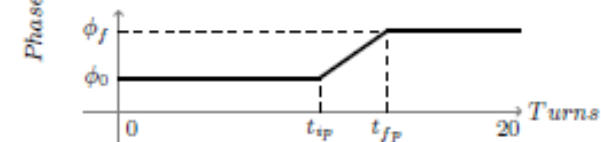
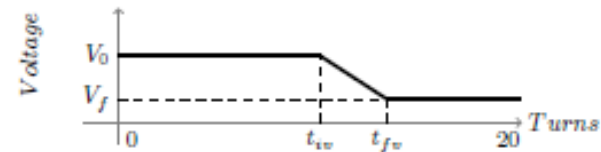
(a) Normal Operation (NO)



(b) Phase failure (PF)



(c) Phase voltage (VF)



(d) Phase and voltage failure (PVF)

Figure 7. The schematic way of changing the voltage and phase through the numbers of turns during the tracking, once the Steady-state is reached.

Results

Tiny halos

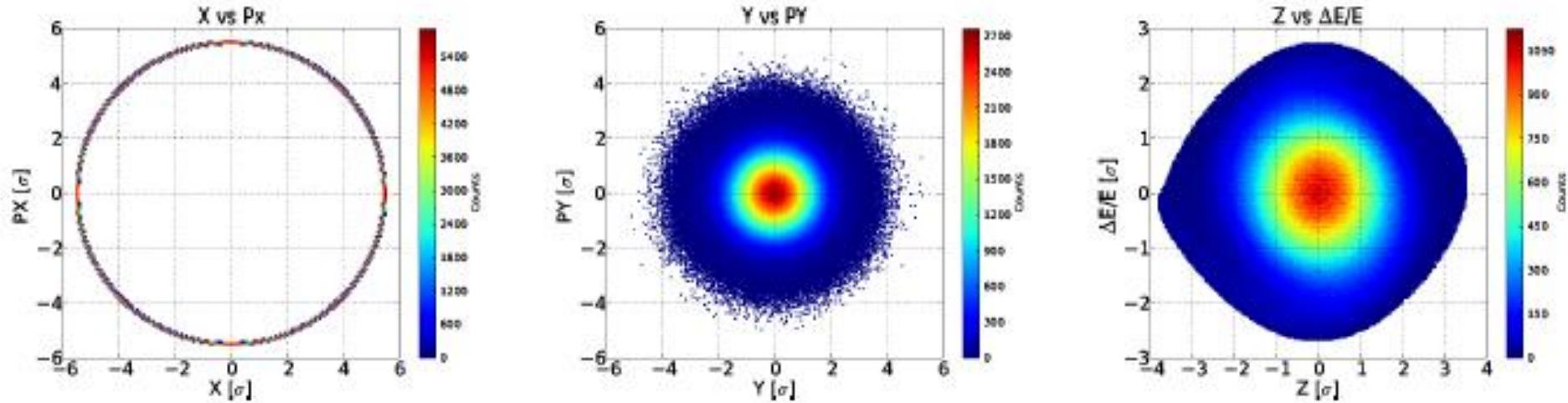


Figure 8 . The phase space using a 2D Gaussian with a tiny horizontal halo at 5.5σ with a smear of 0.1σ . A complete full beam distribution in the vertical and longitudinal phase space.



Percentage of the beam losses for the tiny halos in the collimators

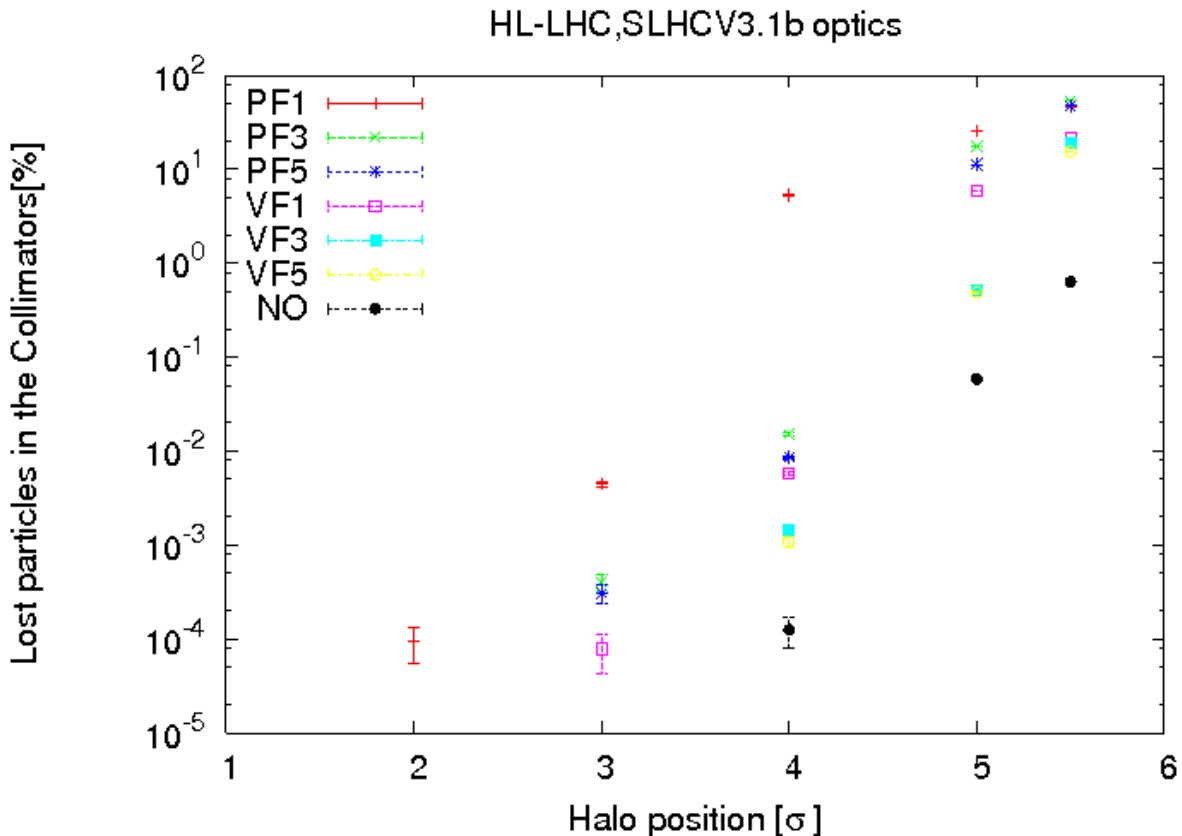


Figure 9 . The percentage of the beam absorbed in the collimators using horizontal halos at different positions with a smear of 0.1σ , for the **PF** , **VF** and **NO** cases.



Percentage of the beam losses for the tiny halos in the aperture

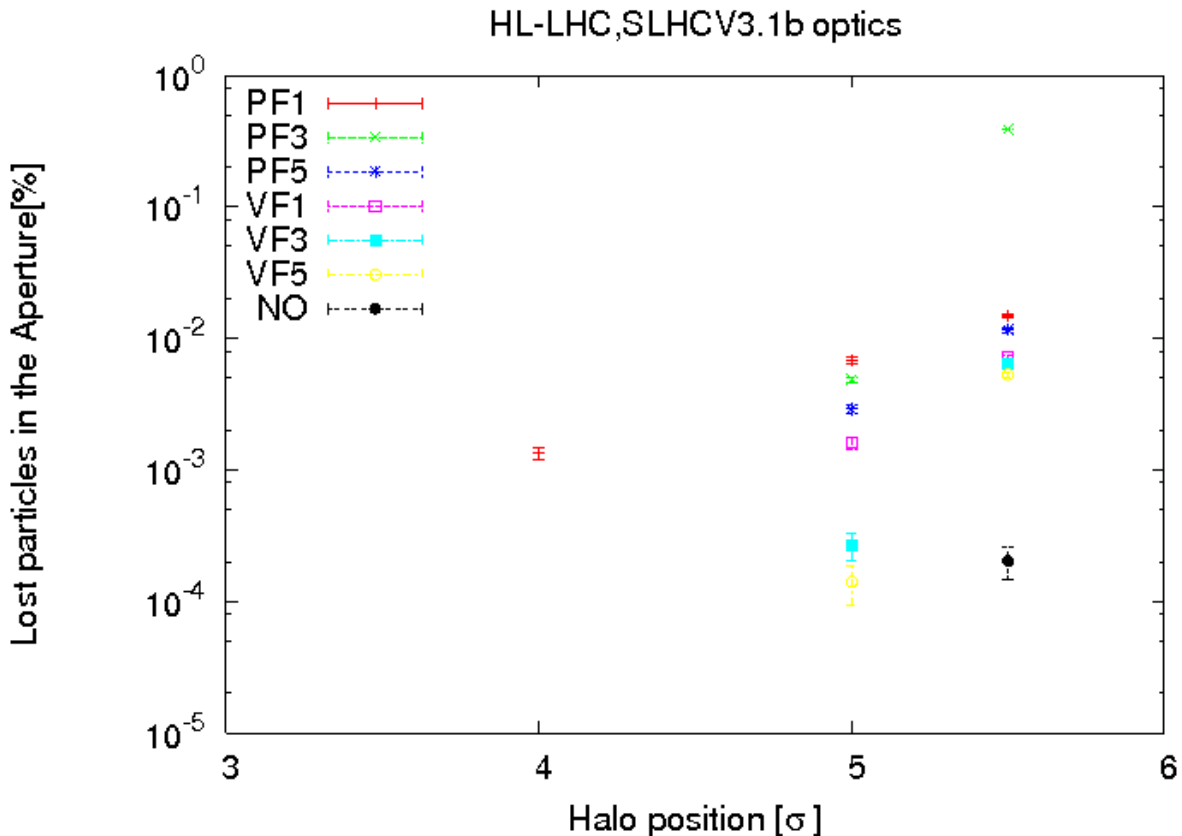


Figure 10 . The percentage of the beam absorbed in the aperture using horizontal halos at different positions with a smear of 0.1 σ, for the **PF VF** and **NO** cases.



Thick distribution phase space I

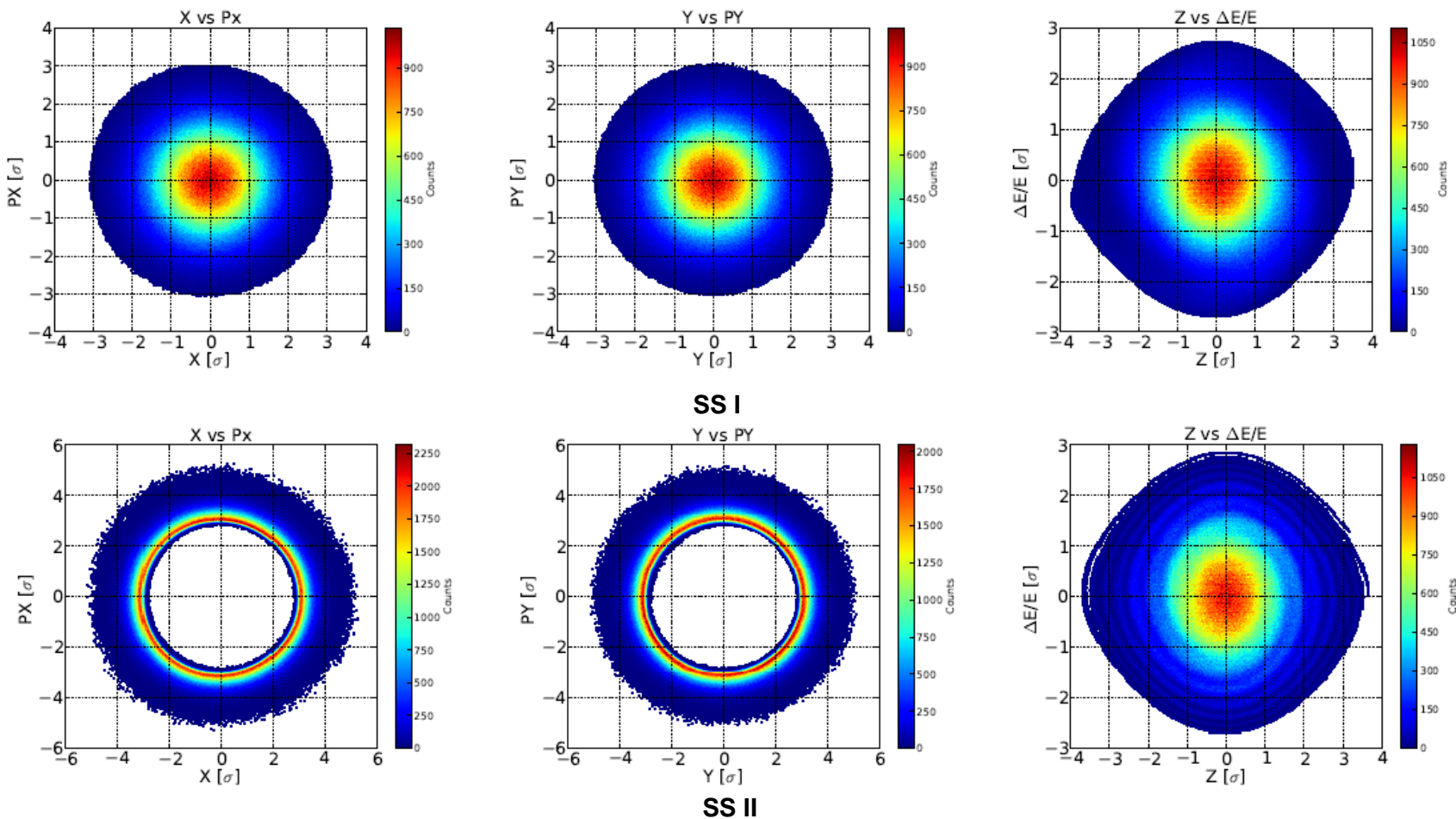


Figure 11. The phase space for the **SS I** and **II**.



Thick distribution phase space II

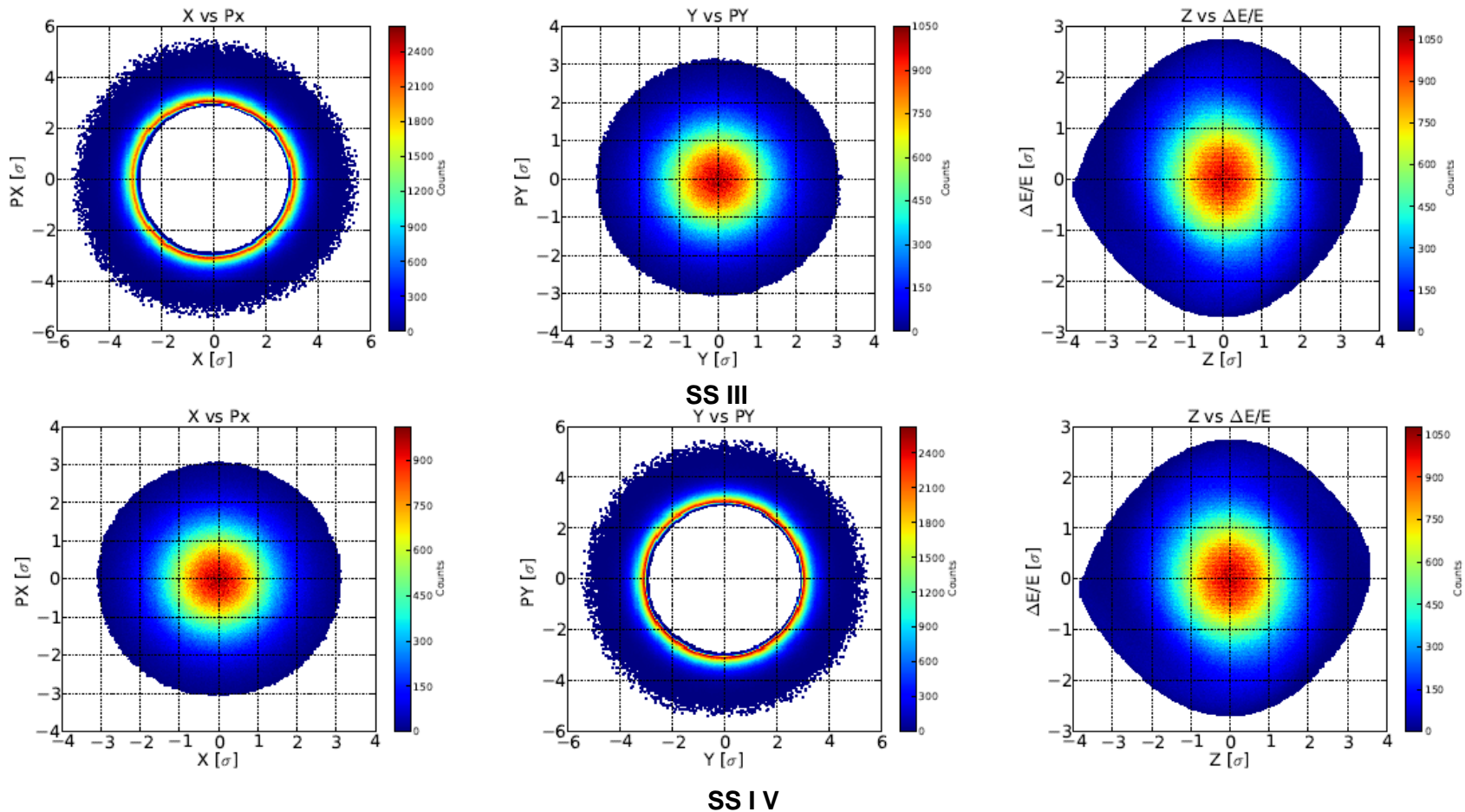


Figure 12. The phase space for the **SS III** and **IV**.
MPP meeting

TABLE III: The equivalent energy stored corresponding to the fraction that represent each **SS** with respect to a HL-LHC full beam*.

SS	% w.r.t. a complete beam	Energy stored [kJ]
I	97.79 ± 0.003	677530.7 ± 20.7
II	1.226 ± 0.017 × 10 ⁻²	84.8 ± 1.1
III	1.100 ± 0.002	7621.2 ± 13.8
IV	1.097 ± 0.001	7600.4 ± 6.9

*Assuming that total stored energy at 7 TeV is 692.84 MJ,.



The percentage of the beam deposited from the SS II

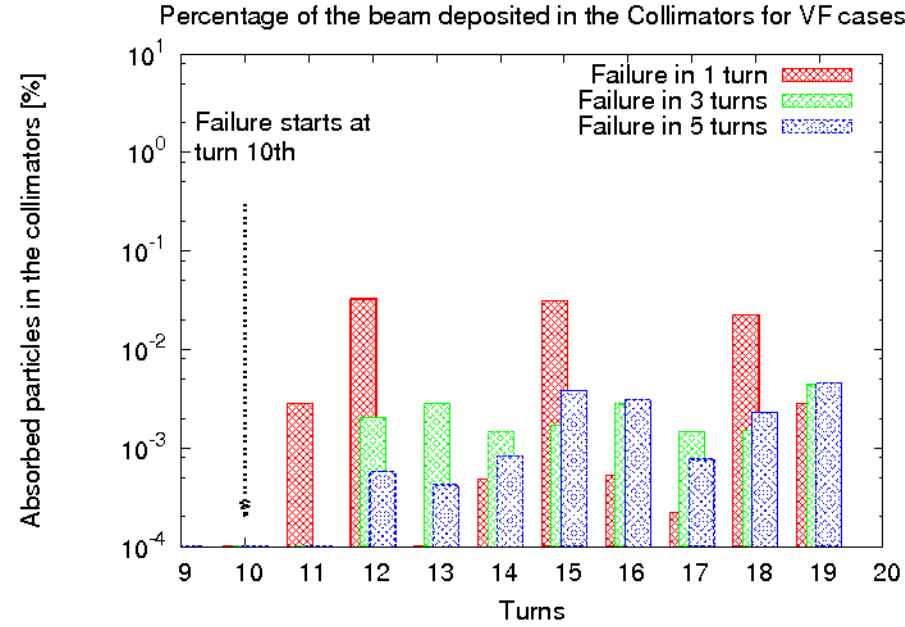
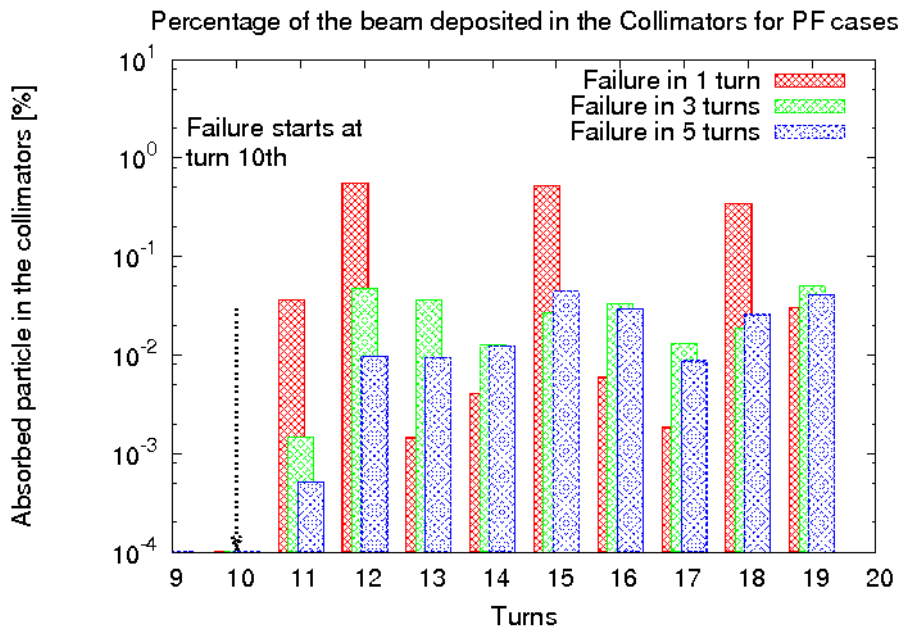


Figure 13. The percentage of the beam deposited turn by turn in the collimators after the failure started for the **PF** and **VF** cases using the **SS II** distributions.



Total beam percentage deposited for the SS II

TABLE IV: The percentage of beam deposited integrated over all the remains turns after the failures for the **PF** and **VF** cases using **SS II** in the aperture and collimators.

Case	Duration of the failure [turns]	Aperture [x 10 ⁻⁵ %]	Collimators [x 10 ⁻³ %]
PF	1	31.97 ± 7.0	1489.3 ± 4.8
	3	10.1 ± 3.9	237.3 ± 1.9
	5	3.1 ± 2.2	180.4 ± 1.6
VF	1	3.9 ± 2.4	93.2 ± 1.2
	3	0	18.2 ± 0.5
	5	0	16.3 ± 0.5



The percentage of the beam deposited from the SS III

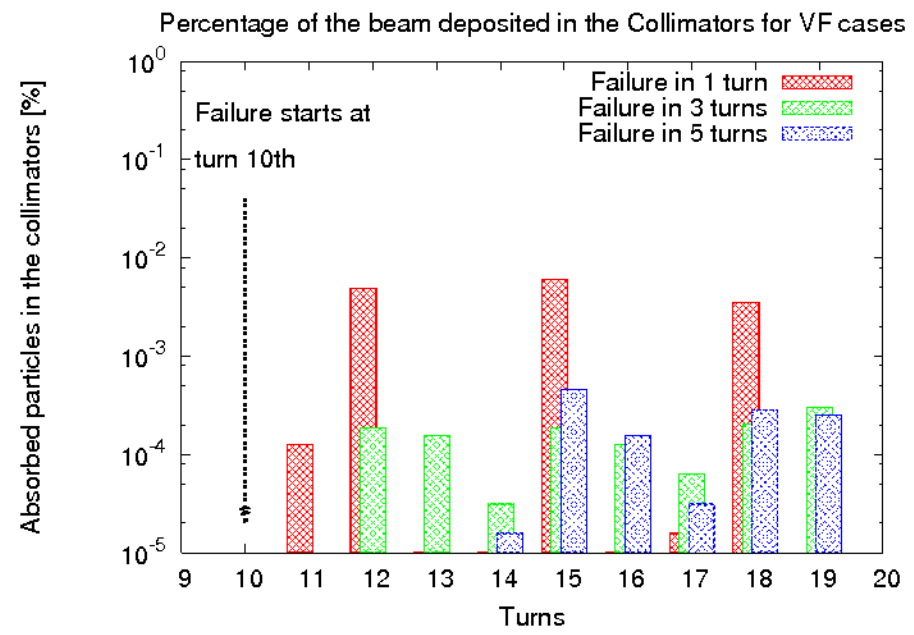
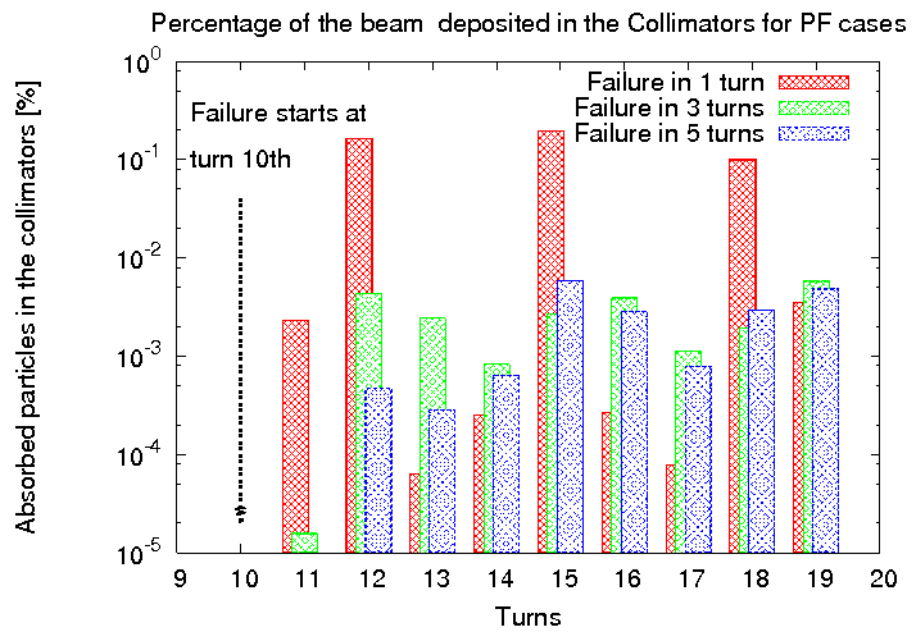


Figure 14. The percentage of the beam deposited turn by turn in the collimators after the failure started for the **PF** and **VF** cases using the **SS III** distributions.

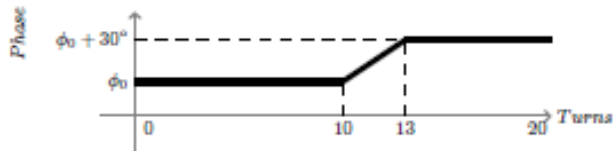
Total beam percentage deposited for the SS III

TABLE V : The percentage of beam integrated over all the remains turns after the failures for the **PF** and **VF** case using **SS III**. Only the **PF** in 1 turn produced beam losses in the aperture of $6.2 \pm 3.1 \times 10^{-5} \%$.

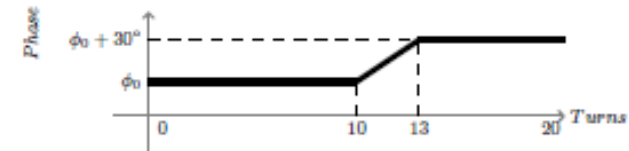
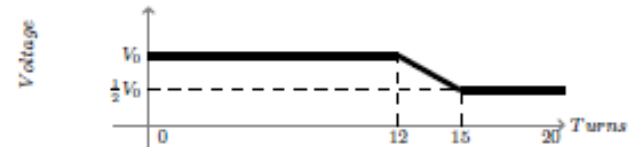
Case	Duration of the failure [turns]	Collimators [$\times 10^{-3}\%$]
PF	1	466.9 ± 2.7
	3	23.0 ± 0.6
	5	18.5 ± 0.5
VF	1	14.6 ± 0.4
	3	1.2 ± 0.1
	5	1.1 ± 0.1

TABLE VI: The percentage of beam deposited integrated over all the remains turns after the failures for the **PF** using **SS IV**. No beam losses were generated for the **VF** cases. In addition, the losses record were just in the collimators.

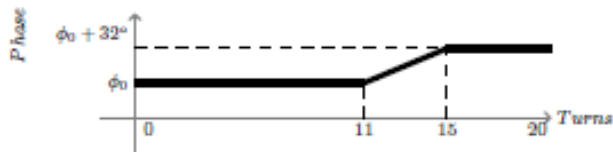
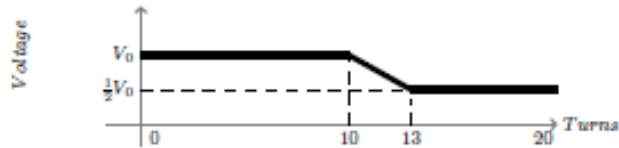
Case	Duration of the failure [turns]	Collimators [$\times 10^{-4}\%$]
PF	1	59.0 ± 3.0
	3	5.3 ± 0.9
	5	3.9 ± 0.7



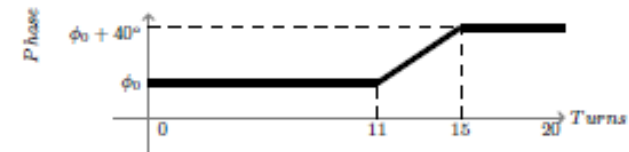
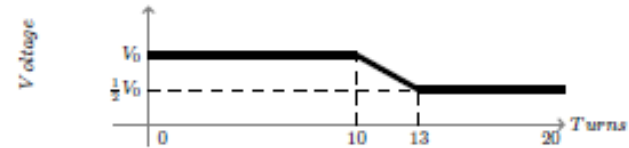
(a) (PVF I)



(b) (PVF II)



(c) (PVF III)



(d) (PVF IV)

Figure 15. The schematic view of the **PVF** failures simulated in this study.

TABLE VII : The percentage of beam integrated deposited over all the 10 turns after the failures for the **PVF** using **SS II** and **SS III** in the collimators. No beam losses were generated for the other **SS** cases. The losses were only in the collimators.

SS	Case PVF	Collimators [$\times 10^{-4}\%$]
II	I	111.8 ± 4.7
	II	103.5 ± 3.5
	III	81.2 ± 3.5
	IV	136.5 ± 4.7
III	I	3.6 ± 0.7
	II	3.5 ± 0.7
	III	2.6 ± 6.4
	IIV	6.4 ± 0.9

TABLE VIII: The Global Inefficiency for the different CCs failures cases. The global inefficiency is the number of the particles lost in the aperture divided by the total lost (in the collimators and aperture). The value for the normal operation of the LHC is 3×10^{-4} using a halo at $6 \sigma^*$.

case	NO [$\times 10^{-4}$]	PF1 [$\times 10^{-4}$]	PF3 [$\times 10^{-4}$]	PF5 [$\times 10^{-4}$]	VF1 [$\times 10^{-4}$]	VF3 [$\times 10^{-4}$]	VF5 [$\times 10^{-4}$]
SS II	-----	2.1	4.2	1.7	2.0	----	-----
SS III	-----	1.8	-----	-----	-----	----	-----
halo 5.5	3.2	3.2	2.5	2.4	3.2	3.4	3.4
halo 5.0	-----	2.6	2.7	2.5	2.6	4.8	2.6
halo 4.0	-----	2.4	-----	-----	-----	-----	----

*A. Marsili. Collimator alignment error models in SixTrack, ColUS Meeting, Nov 2013

LLM for the SS II

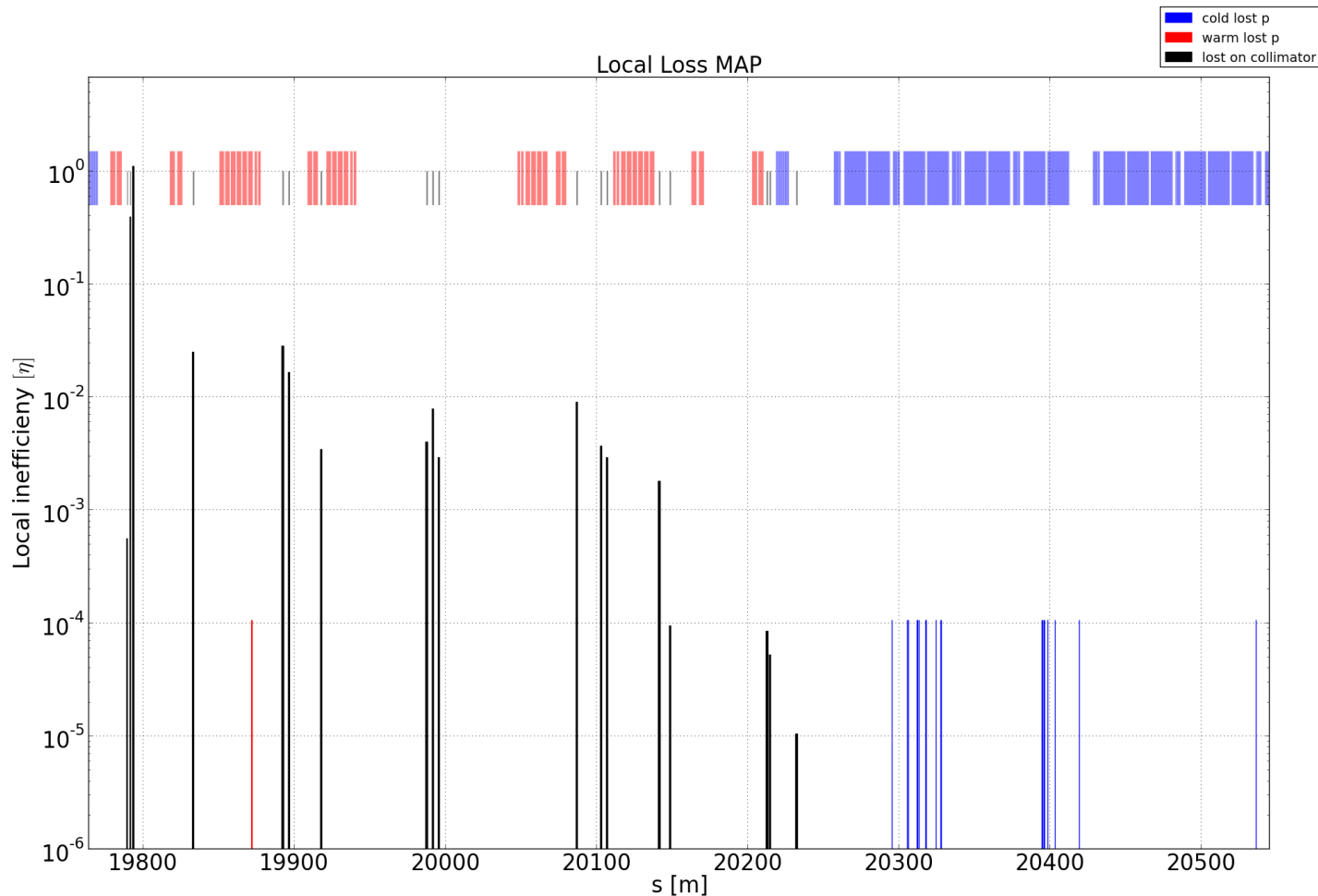


Figure 16. The Local loss Map using the **SS II**, for the **PF** in 1 turn close up at IR7.

LLM for the SS III

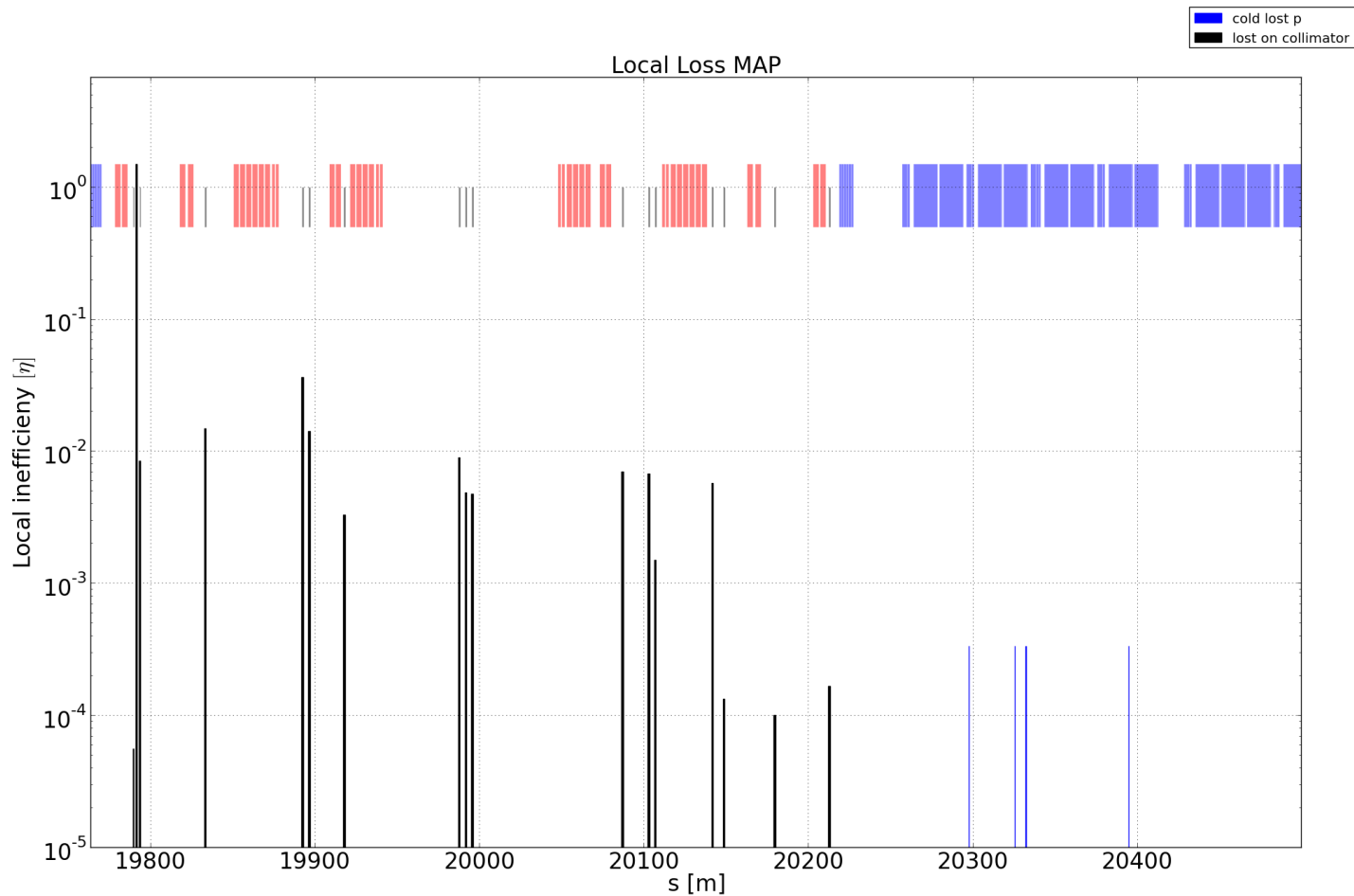


Figure 17. The Local loss Map using the **SS III**, for the **PF** in 1 turn close up at IR7.

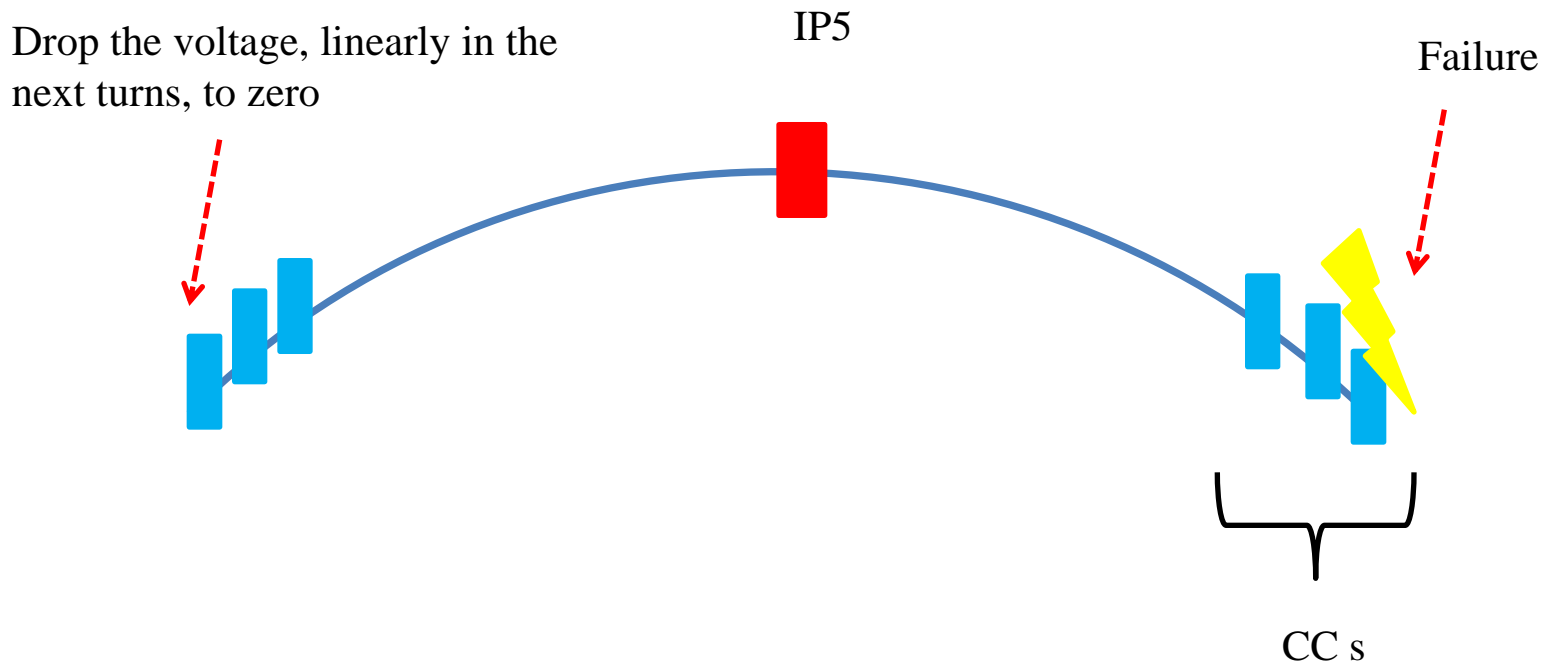


Figure 18. The scheme layout for mitigation cases . In case the voltage failure the CC that close the bump will drop to zero. Indeed, for phase failure the voltage of the CC which fail and the one which close the bump, both will drop to zero.

Mitigation results

TABLE IX : The percentage of reduction of the beam loss for the **PF** and **VF** cases using the **SS II** and **SS III** in the collimators after applications of the mitigation strategies. In these simulations the mitigation started one turn after the failure is produced and took 3 turns to drop the voltage to zero.

SS	CC failure cases	Duration of the failure [turns]	Reduction of the Beam loss [%]
SS II	PF	1	~81
		3	~90
	VF	1	~75
		3	~95
SS III	PF	1	~90
		3	~95
	VF	1	~86
		3	~98

Dropping linearly the voltage in 9 turns the beam reduce ~71% for the PF1 in SSIII .

Dropping exponentially the voltage ($\tau= 9$ LHC turns) in 9 turns the beam reduce ~65% for the PF1 in SSIII .

Summary

Summary I

- This study present the first results of the CCs using a more realistic steady-state in the LHC.
- The SSII and SS III represent the most interesting cases , cause they are the ones with tails distribution in the horizontal plane. The SS III represent more percentage of the full beam than SS II.
- Previous studies of the quench test (2013) show that highest load in the TCP is 100 kW during 10 s, which mean 1 MJ. In order to have upper limit for the energy deposited in the collimators for our simulations, we can assume that all the energy of the particle which impact in the collimator was deposited , therefore, in the worst case (for PF1 using SIII) , we deposited 10 k J over a time of 100 μ s.

Summary II

- Assuming that:
 - a) The material properties of the collimators remains constant between room temperature and 150° C .
 - b) Neglecting the thermal diffusion.
 - c) For the same FLUKA map.
- And remembering the dynamic stresses peaks can be considered around 2 times larger than the static stresses *. This case would induce a maximum stress of the 2% of the material elastic limit **. However, Fluka studies are required to calculated the energy deposited in the collimators.
- A FLUKA calculations for the peak energy density in coils is need it to asses the damage in the magnets***. The energy necessary to quench a standard magnet is around 20 mJ/cm³

*A. Bertarelli et al. “THERMALLY INDUCED VIBRATIONS OF BEAMS: LONGITUDINAL AND FLEXURAL BEHAVIOUR”, Journal of Applied mechanics.

** private communication by F. Carra and R. Bruce

***Private Communication with A. Lechner and D. Wollmann.

Summary III

- The global inefficiency for the normal LHC performance is 3×10^{-4} . In the Crab Cavities the value obtained for the Steady-State and their failures are in the order of 10^{-4} . Therefore, the CCs do not increase dramatically the global inefficiency in the LHC.
- For the abrupt CCs failures the beam losses simulated remains in the threshold of safety operation. Nevertheless, the population in our beam tails were 0.03 % ($> 4\sigma$). In the LHC overpopulate tails were observed 5 %*. This represent 2 order of magnitude higher in the energy deposited (at least on collimators) that will represent a serious threat for the LHC lattice.

* F. Burkart, Halo Scraping with collimators in the LHC, CERN-AB-NOTE-2004-054(ABP), 2004.

Acknowledgments

- J. Barranco, F. Bouly, R. Bruce, R. Calaga, F. Carra, A. Lechner, A. Marsilli, D. Wollmann, F. Zimmermann for the comments and discussions.
- To US-LARP and Conacyt for the support this project.

Thanks for you attention

Backup

TABLE X: The Collimators settings used for the HL-LHC studies . Similar to Collimation team settings*, the only difference is that they have open the TCLP and TCLI.

Collimators	Nominal opening [σ]	Collimators	Nominal opening [σ]
TCP IR7	6	TCLP	12
TCSG IR7	7	TCLI	10
TCLA IR7	10	TCSTCDQ IR6	7.5
TCP IR3	12	TCDQ IR6	8
TCSG IR3	15.6	TDI	Open
TCLA IR3	17.6	TCT IR1/IR5	8.3
		TCT IR2/IR8	30

*A. Marsilli et al. Collimation cleaning with ATS optics for HL-LHC, Collimation Review, May, 2013.

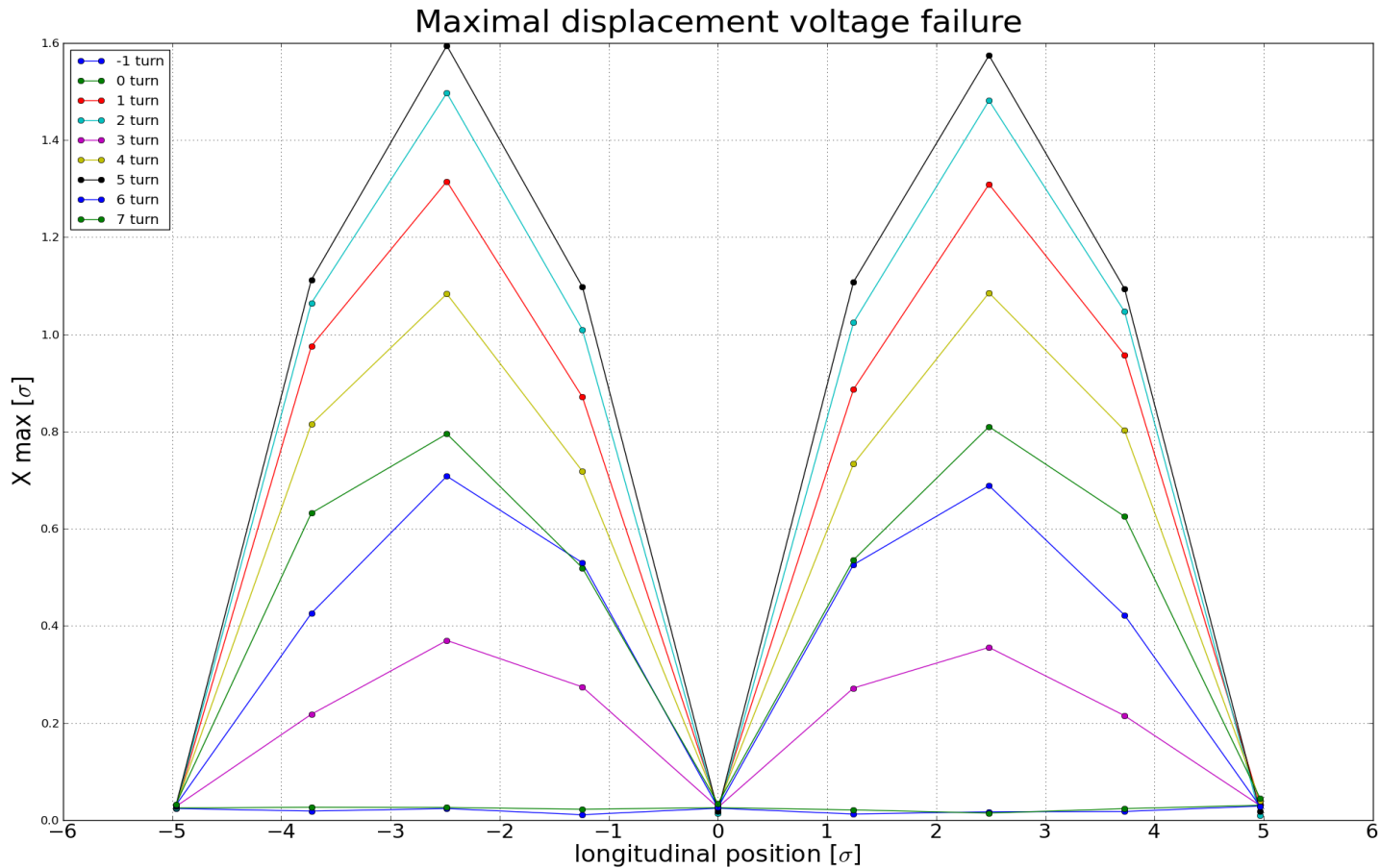


Figure 19. The maximal transverse displacement produced by a failures of one CC voltage that close up the bump for particles at different longitudinal positions. The failures begin in the turn 1.